Dalton Transactions

Accepted Manuscript

ROYAL SOCIETY OF CHEMISTRY

www.rsc.org/dalton

Speciation of americium in seawater and accumulation in marine sponge *Aplysina cavernicola*.

*Melody MALOUBIER[a,b], Hervé MICHEL[a] , Pier Lorenzo SOLARI[c], Philippe MOISY[d], Marie-Aude TRIBALAT[a] , François R. OBERHAENSLI[e], Marie Yasmine DECHRAOUI BOTTEIN[e], Olivier P. THOMAS[a], Marguerite MONFORT[b], Christophe MOULIN[b**], Christophe DEN AUWER[a*]*

[a] University of Nice Sophia Antipolis, Nice Chemistry Institute UMR CNRS 7272, 06108, Nice, France ([*] christophe.denauwer@unice.fr)

b CEA, DAM, DIF, F-91297 Arpajon, France ([**]christophe.moulin@cea.fr)

c Synchrotron SOLEIL L'Orme des Merisiers, Saint-Aubin, BP 48, F-91192 Gif-sur-Yvette Cedex, France

[d] CEA, Nuclear Energy Division, RadioChemistry & Processes Department, BP17171, F-30207 Bagnols sur Cèze, France

[e] *IAEA, Environment Laboratory, 4 Quai Antoine Ier, MC-98000, Monaco*

Abstract

The fate of radionuclides in the environment is a cause of great concern for modern society, seen especially in 2011 after the Fukushima accident. Among the environmental compartments, seawater covers most of the earth's surface and may be directly or indirectly impacted. The interaction between

radionuclides and the marine compartment is therefore essential for better understanding the transfer mechanisms from the hydrosphere to the biosphere. This information allows for the evaluation of the impact on humans via our interaction with biotope that has been largely undocumented up to now. In this report, we attempt to make a link between the speciation in natural seawater and uptake by a model marine organism. More specifically, because the interaction of actinides with marine invertebrates has been poorly studied, the accumulation in a representative member of the Mediterranean coralligenous habitat, the sponge *Aplysina cavernicola,* was investigated and its uptake curve exposed to a radiotracer ^{241}Am was estimated using a high-purity Ge gamma spectrometer. But in order to go beyond the phenomenological accumulation rate, the speciation of americium(III) in seawater must be assessed. Speciation of ^{241}Am (and natural europium as its chemical stable surrogate) in seawater was determined using a combination of different techniques: Time-Resolved Laser-Induced Fluorescence (TRLIF), Extended X-ray Absorption Fine Structure (EXAFS) at the L_{III} edge, Attenuated Total Reflectance Fourier Transform Infrared spectroscopy (ATR-FTIR) and Scanning Electron Microscopy (SEM) and the resulting data were compared with the speciation modeling. In seawater, the americium(III) complex (as well as the europium corresponding complex, although with conformational differences) was identified as a ternary sodium biscarbonato complex, which formula can be tentatively written as $NaAm(CO_3)_2.nH_2O$. It is therefore this chemical form of americium that is accumulated by the sponge *A. cavernicola*.

1.1. Introduction

Major sources of radionuclides in the environment, except for uranium and thorium, are anthropogenic. Among the causes of human dissemination, nuclear weapons tests and industrial accidents have been the most investigated for the release of non-negligible quantities of radionuclides in the environment. Nuclear weapons tests in the 60s mainly occurred in the northern hemisphere with fallout across the globe. Later, in 1986, the Chernobyl accident led to an atmospheric release affecting mainly Europe [1, 2]. The more recent accident of Fukushima was more confined but it also involved dissemination (although estimates to

date indicate only minor amounts) of radionuclides in seawater [3-5]. In the case of such nuclear contamination, seawater could become the ultimate receptacle, whether the accident occurs on a sea shore (like the Fukushima accident) or further away from, but connected to the sea *via* the rivers system. In the case of Fukushima, seawater was the ultimate receptacle and it was also injected into the high-temperature reactor for cooling[4]. Moreover, more than 10^{19} Bq of radionuclides were released into the environment during the accident, leading to a concentration of ^{236}U about 10^{6} atoms/kg. The amount of radionuclides released directly into the sea has been estimated to 2.3 – 26.9 PBq[6]. Furthermore, among the environmental compartments, seawater is the most abundant and one of the most complex systems because of its intricate composition (anions, cations, organic matter), heterogeneity (as a function of depth for instance) and mobility (streams). In order to establish a model for understanding the radionuclide dispersion in seawater and to evaluate the impact on humans, many parameters must be taken into account such as the current fields, the advection and diffusion, exchange between waters and suspended matters, winds and ocean acidification, for example[7].

In the marine environment, the bioaccumulation of inorganic contaminants has already been described in occurrence with organisms from all trophic levels such as algae, mussels, fish and sponges which have been proposed as potential sentinel biomonitors for metallic pollution [8-12]. This report is part of our effort to make a link between the speciation of heavy elements (radionuclides) in natural seawater and uptake by marine organisms in order to further understand the biochemical transfer mechanisms.

Among these organisms, sponges are immobile active filter feeders and have been identified as hyper accumulators of several heavy metals [13-16]. Several studies have shown that sponges are a proper bioindicator of trace metals. The Indian sponge *Spirastrella cuspidifera* accumulates, for example, Cd, Cr and Sn up to concentration 5 to 7 orders of magnitude higher than in water [14]. The accumulation of metals in sponges is highly dependent on the species. Indeed, out of four Mediterranean species, only three were shown to be an appropriate copper bio indicator: *Crambe Crambe, Phorbas tenacior* and *Dysidea avara* [16]. The Mediterranean sponge *Aplysina cavernicola* [17] was selected in this study as a bioaccumulator of radionuclides in marine organisms [18]. This sponge is commonly found in the

entrance of the caves off the coasts of the Northwestern Mediterranean and previous preliminary tests have shown that it has a substantial capacity for metal accumulation. Sponges may also be proper candidates as sentinel or for the bioremediation of such elements in this particularly complex medium. This possibility would be of great importance for the treatment of contaminated seawaters in case of accidental release as in the Fukushima accident for the water compartment [19]. However, the accumulation mechanisms are still unknown and depend i) on the speciation in seawater and ii) on the biochemistry involved upon uptake by the sponge. In this study, only the speciation in seawater will be discussed.

For radionuclides disseminated in seawater, an approach based on tabulated complexation constants and predictive speciation diagrams has been reported [20-22]. This approach is a useful guide to better describe the molecular speciation but lacks experimental data involving an experimental speciation approach. Although the inventory of radionuclides, including actinide elements (uranium, plutonium, americium …), has been widely studied in the geosphere, speciation has been difficult to assess, mostly because those elements are present at ultra-trace levels (below the ppb level) in the absence of hot contamination spots. Concentration assessments of these radionuclides have been generally performed with alpha, gamma nuclear radiometry or analytical techniques such as inductively coupled plasma mass spectrometry (ICP-MS) or accelerator mass spectrometry (AMS) whose sensitivity is often below 10^{-8} M depending on the isotopes [23]. In the specific case of seawater, the very high complexity of the medium (with its high salinity) makes ICP-MS, which is considered a very sensitive analytical technique, often difficult to implement without prior sample preparation. Nevertheless, to study the impact of the Fukushima accident on seawater, an isotopic determination of U, Pu and Cs has been achieved by AMS, ICP-MS and γ-ray spectrometry [24]. Several studies also showed the need to perform coprecipitations or separations method to determine the actinide concentrations (U, Pu) in seawater by ICP-MS or α-spectrometry [21, 25, 26]. In any case, these methods do not lead to any information on their speciation, key data in order to assess the real impacts of these elements on marine organisms. On the other hand,

direct molecular probes have only rarely been used because no spectroscopic technique is able to be sensitive to such a low level of concentration[27]. As a consequence, very little is known about the speciation of actinides in seawater. However, the speciation of actinides might modify their toxicity and their bioavailability. Hence, in the case of uranium, it has been shown, for instance, in Finnish mineral water that the two occurring mixed complexes $Ca_2[UO_2(CO_3)_3]$ and $Ca[UO_2(CO_3)_3]^{2-}$ are non-toxic since they are not bio-available [28, 29]. This example demonstrates, that knowledge about speciation and chemical mechanisms is essential to better understand the transfer mechanisms from the hydrosphere to the biosphere and to evaluate their global impact on the environment. In a previous paper [30] a methodology to circumvent those difficulties and to allow direct speciation studies has been presented for uranium and neptunium. It involves the doping of natural seawater by the cation of interest below the concentration of the major ions but above the detection limit for spectroscopy. This is clearly a compromise between the use of model systems and direct environmental probing that is often inaccessible to spectroscopy.

Americium(III) was chosen for this study as a representative of the heavier trivalent actinides such as curium about which very few data (if any) are available. It is also an element with a relatively simple RedOx chemistry compared to uranium, neptunium and plutonium. For the reasons described above as well as in our previous report [30], concerning the study of the speciation of americium in seawater, seawater samples were doped at $5x10^{-5}$ M because this value is a compromise between a suitable concentration for EXAFS (Extended X-ray Absorption Fine Structure) data acquisition and the less intrusive doping concentration as explained in the experimental section. Because of the relatively high specific radioactivity of available 241- and 243-Am, complementary model systems are difficult to handle. For that reason a parallel investigation was also conducted on europium (a stable lanthanide with chemical properties very close to that of americium [23, 31]). Although the solubility limit of europium is reached at this concentration ($5x10^{-5}$ M) in seawater it remains a very useful chemical surrogate for comparative model studies in seawater as well as in the solid phase. The combination between speciation modeling and spectroscopy being the only way to cast light on the speciation of americium, the following

techniques have been implemented : for americium in seawater, EXAFS; for europium in seawater, EXAFS and TRLIF (Time-Resolved Laser-Induced Fluorescence); for europium model compounds in the solid phase, FTIR (Fourier Transformed Infra-Red) and SEM (Scanning Electron Microscopy).

Time-Resolved Laser-Induced Fluorescence (TRLIF) first is a very sensitive and selective method for several fluorescent actinides (U, Am, Cm) and lanthanides (Eu, Tb, Dy, Sm) in various fields (nuclear, geological, environmental and medical chemistry) widely used for speciation studies [32-35]. Additionally, EXAFS is a local spectroscopic probe able to characterize the atomic environment (closest atoms, interatomic distances…) of the element investigated. However, EXAFS is not a sensitive technique. Consequently, EXAFS studies are usually performed at the mM level even if it has gone down to the µM level in scarce examples. Attenuated Total Reflectance FTIR (ATR-FTIR) is often used to study the molecular coordination environment of the cation in solid or solution (mM level). For instance, this technique allows for the determination of the metal carbonate coordination mode: monodentate or bidentate [37, 38] in model systems, as in the case of europium. Finally, in order to obtain more information about the morphology and the composition of the europium models, a SEM equipped with an Energy Dispersive X-ray analyzer was used.

2. Experimental

2.1. Materials and sample preparation

Seawater samples were collected in the Mediterranean Sea by the Environmental Laboratory of IAEA at 30 m off the coast of Monaco at 30 m depth (43° 43′ 49″ N, 7° 25′ 40 ″ E). The seawater was filtered at 0.2 µm (Whatman, GF/C grade) and sterilized by UV treatment in order to eliminate particles and microorganisms.

Seawater sample solutions were prepared by doping at [Eu(III), Am(III)] = $5x10^{-5}$ M. The pH of the solution was measured with a conventional pH meter (Model PHN 81, Tacussel) equipped with a subminiature combined electrode (Model MIXC710).

2.1.1. Europium

An amount (approximately 12.0 mg) of europium nitrate was dissolved under N_2 dry atmosphere in a large volume (500 ml) of seawater (pH = 7.8) to reach the concentration around $5x10^{-5}$ M. ICP-OES measurement after suitable dilution confirmed a concentration of $(5.4\pm0.3)x10^{-5}$ M. At this concentration, a colloidal solution appeared quite readily in seawater leading to a precipitate after a few days. This is not surprising considering that the log Ks given in literature data are for instance -20.9 for $NaEu(CO_3)_2$ to zero ionic strength and -31.78 for $Eu_2(CO_3)_3$[39, 40]. In the following text the distinction between the "solid phase" and the "soluble phase" of europium in seawater will therefore be made. In order to analyze this solid phase, another solution was prepared in the same conditions and the solid was removed by centrifugation at 4000 rpm for 1 hour and washed with water. A partial elementary measure was made by ICP-OES (Perkin-Elmer Optima 2000 DV) giving a 1:1 ratio of Eu:Na. The solid phase was also characterized by ATR-FTIR comparing to $Eu_2(CO_3)_3.nH_2O$ (synthesized by precipitation of a solution of europium nitrate ($5x10^{-3}$ M) with carbonates (under 100% CO_2 atmosphere) in $NaClO_4$ 0.1 M [39, 41]) and to an unidentified europium carbonate (synthesized by adding 12.0 mg of europium nitrate and 92.8 mg of $NaHCO_3$ $2.3x10^{-3}$ M, Prolabo, in NaCl 0.7 M). All solids were centrifuged and dried at 35°C. The ATR-FTIR spectra were recorded in the range 4000-400 cm^{-1} (resolution: 4 cm^{-1}, 64 scans per spectrum) on a spectrometer Tensor 27 (Bruker) with a single reflection ATR MVP Pro (Harrick) module. Furthermore, the seawater doped solution was analyzed by Scanning Electron Microscopy (SEM) after drying. An FEI Quanta 3D FEG was used to image seawater particles after their deposition on a carbon disk. This instrument is equipped with an EDX analyzer (EDAX).

2.1.2. Americium

Americium-241 was obtained from the CEA inventory. Americium is a radioactive element and was handled in dedicated glove boxes. The solution was prepared from a purified solution of ^{241}Am (1.85mM) in nitric acid (conc.). The solution was evaporated at 200°C, then dissolved in hydrochloric acid (0.1 M) and evaporated twice again. The solid obtained was dissolved in seawater to obtain a concentration of $5x10^{-5}$ M. (600µl)

In the case of americium, no colloidal solution was observed after the solution preparation, the entire fraction is therefore soluble.

2.1.3. Biological material

Two specimens of the Mediterranean sponge *Aplysina cavernicola*, a tubular yellow sponge with a spongine skeleton, were collected by SCUBA diving at a 25 m depth in the entrance of a cave off the coast of Saint-Jean-Cap-Ferrat (France, 43° 41′ 29″ N, 7° 19′ 11″ E). Individuals of homogeneous size, with an average length close to 3.0 cm and an average diameter of 1.4 cm, were selected.

2.2. Sponge bioaccumulation with americium-241.

A stock solution of ^{241}Am radiotracer (2.15 kBq/g in 0.01 N HCl) was used. Before the uptake experiments, two specimens were acclimated for a few days in a 20 l aquarium. For the uptake measurements, a contamination cycle was performed every day according to the following procedure: for 9 h, sponges were maintained in an open water system; then, the sponges were placed in 735 ml boxes in the same aquarium, and maintained in a closed water system. The radiotracer was spiked by the addition of 30 µl of the stock solution in the seawater corresponding to an activity of 64.5 Bq in ^{251}Am; after 15 hours exposure, the system was opened for sponge recovery. This cycle was repeated 5 times. In order to assess potential americium adsorption on the boxes, a blank test consisting of fusing an empty 735 ml box was performed. The uptake curve was obtained using gamma radiometry. At the end of each 15h spike sequence, 50 ml of seawater were taken off the 735 ml box and the associated radioactivity was measured by gamma spectrometry. The difference between the spiked activity and the measured activity after the 15h spike sequence indicated potential uptake by the sponge.

The gamma emission of ^{241}Am was assayed at 59.5 keV using a high resolution γ spectrometer with a coaxial high purity germanium (HPGe) detector (ORTEC GEM 100 - 95). Counting time was adjusted to obtain counting errors below 10%. The blank test revealed that less than 0.5 Bq were adsorbed on the plastic boxes during the entire procedure. At the end of the experiment, the sponges were collected and rinsed in clean seawater to remove radiolabeled water from the aquifer system.

2.3. Modeling and doping concentration

Speciation calculations were processed with JCHESS software for americium and europium [42]. Thermodynamic data used for calculation arose from the database BASSIST [43, 44] (Base Applied to Speciation in Solution and at Interfaces and Solubility Thermodynamic database) for europium and from the database NEA for americium which were taken from the NEA-OECD [23] . The equilibrium constants considered in the calculations involving elements at significant concentrations in seawater are reported in Table S1 and S2 of Supplementary Information for americium and europium respectively. Seawater composition was defined with concentrations measured directly from the seawater collected in Monaco (Table 1) and with concentration of minor ions and metals taken from literature data (Table S3). For the metal concentrations in seawater average values were used because they are location and depth dependent [45-55].

In order to assess the impact of doping on the complexation equilibria for Am and Eu at environmental concentrations (10^{-17} M), speciation modeling diagrams in these conditions were compared to diagrams at doping concentration ($5x10^{-5}$ M) (Figure S4 and S5). No difference was observed in speciation between the environmental concentrations and doping concentration. However, modeling speciation has significant limitations and can only be helpful to obtain an initial estimation of the speciation. Indeed, most speciation models assume equilibrium conditions and use only thermodynamic data without taking into account the kinetic. Furthermore, even when seawater is doped, the europium and americium concentrations are still below the main ion concentrations (in particular carbonates). Concerning other species like nitrate, concentrations are low (1.8 µM) and complexation constants are lower compared to those of the major anions present in seawater [23]. Furthermore, in each case the amount of anion (Cl^- or NO_3^-) introduced in seawater during sample preparation is insignificant in comparison with the natural anion concentration (the quantity of nitrate and chloride introduced is equal or less to 0.026 % of the total ionic strength).

2.4. Time-Resolved Laser-Induced Fluorescence Spectroscopy

A Nd-YAG laser (Model Surelite Quantel) operating at 355 nm (tripled) and delivering about 10 mJ of energy in a 10 ns pulse with a repetition rate of 10 Hz, was used as the excitation source for europium. The speciation of americium was not studied by TRLIF because the detection limit is higher (10^{-6} M) the high specific activity requires a specific installation. The laser output energy was monitored by a laser power meter (Scientech). The focused output beam was directed into the 4 ml quartz cell and into the 0.35 µl quartz cell for solid samples of the spectrofluorometer (F900-Edinburgh). The detection was performed by an intensified charge coupled device (Andor Technology) cooled by Peltier effect (-5°C) and positioned at the polychromator exit for the emission spectra measurement and by a photomultiplier tube (PMT) to measure fluorescence decay time. Logic circuits, synchronized with the laser shot beam, allowed the intensifier to be activated with determined time delay (from 0.005 to 1000 µs) and during a determined aperture time (from 0.005 to 1000 µs). From a spectroscopic point of view, various gate delay and duration were used to certify the presence of only one complex by the measurement of a single fluorescence lifetime and spectrum. The fluorescence spectra and fluorescence decay curves were analyzed using the software ORIGIN 8.0. All peaks were described using a mixed Gaussian-Lorentzian profile. Fluorescence lifetime measurements were made by varying the temporal delay with fixed gate width. Europium(III) doped seawater at $5x10^{-5}$ M and the precipitate obtained were measured and compared with the carbonate free solution.

2.5. Extended X-ray Absorption Fine Structure

EXAFS experiments at the Eu and Am L_{III} edge were carried out on the MARS beamline of the SOLEIL synchrotron facility. The MARS beamline is devoted to the investigation of radioactive materials in the hard X-ray range [56, 57]. The optics of the beamline essentially consist of a water-cooled double-crystal monochromator (FMB Oxford), which is used to select the incident energy of the X-ray beam and for horizontal focalization, and two large water-cooled reflecting mirrors (IRELEC/SESO) that were used for high-energy rejection (harmonic part) and vertical collimation and focalization. In this case, the monochromator was set with the Si(111) crystals and the mirrors with the Si strips and with the Si(220) crystals and the mirrors with the Pt strips for europium and americium, respectively. Energy calibration

was performed at the Fe K edge at 7112 eV for europium and at Zr K edge at 17998 eV for americium. EXAFS measurements were performed in fluorescence mode, due to the low concentration, using a 13-element high purity germanium detector (ORTEC).

Data processing was carried out using the Athena code [58]. The e_o energy was identified at the maximum of the absorption edge. The EXAFS signal was extracted in three steps: the subtraction of a linear pre-edge background, the removal of cubic spline functions for atomic absorption background and normalization. Fourier Transformation (FT) in k^2 was performed between 2.51 and 9.83 $Å^{-1}$ with Hanning windows using the ARTEMIS code [58]. Spectral noise was calculated using the CHEROKEE code [59, 60] by using the Fourier back transform filter above 6 Å corresponding to the noise spectrum. The r factor (%) and the quality factor (QF, reduced χ^2) of the fits were provided by ARTEMIS. The fitting procedure was optimized using europium solid phase carbonate models. Phases and amplitudes were calculated using the FEFF9 simulation code [61] using i) the simple scattering approach with Eu-O and Eu-Na paths (Eu-C path is not visible) and ii) multiple scattering approach using a triple scattering path for the bidentate carbonate ligands (Eu...C-O_{dist} path with O_{dist} = distal oxygen of the carbonate), and a quadruple scattering path for the monodentate carbonate ligands (Eu...C-O_{dist}-C path). The structural parameters of the multiple scattering paths were linked to those of the corresponding single scattering paths in order to reduce the number of free parameters. The same methodology and same paths were applied to the case of americium with Z=63 replaced by Z=95 in the FEFF9 input file.

3. Results and discussion

As mentioned in the introduction, marine sponges are known to accumulate high amounts of metals ranging from copper to lead with no specificity of their chemistry (oxidation state, hard, soft cations etc...) [13-16, 62-64]. In the following section, we first report the uptake of americium(III) at the ultra-trace scale by *A. cavernicola.* No description of the sponging up biochemical mechanisms is made because it is far beyond the scope of this work and such study would be extremely limited by the high specific activity of americium. In a second step, the molecular speciation of americium in natural seawater is fully discussed, in comparison with europium as a model element.

3.1. Americium bioaccumulation in sponges

In order to test the accumulation ability of *A. cavernicola* for actinide(III) at the ultra-trace range, the uptake curve of radiotracer ^{241}Am was been recorded. Because the experiment was carried out at the ultra-trace scale, no saturation effect, if accumulation occurs, was expected. In Figure 1, two sponges were exposed in parallel to 64.5 Bq every day for 15h per day, corresponding to an amount of [^{241}Am(III)] = $3x10^{-12}$ M (0.72 pg/ml) in seawater. Throughout the entire experiment, 5 spikes (5 days) were performed corresponding to a total of 323 Bq over the course of the experiment (2543 pg). For each specimen, the americium concentration in the sponge increases linearly without reaching a steady state. The accumulation rate is close to 100 %. This means first of all that the americium under the present speciation (see next section) was accumulated and not rejected by the sponge. At the end of the experiment, the measurements carried out on seawater samples indicated that the maximum amount of americium within the two sponges was equal to 2.5 $x10^{-12}$ mol/g and 3.2 $x10^{-12}$ mol/g (calculated for dry weight). Americium accumulation has already been studied by Genta-Jouve *et al.* in different Mediterranean sponges: *Chondrosia reniformis*, *Agelas oroides*, *Ircinia variabilis*, *Acanthella acuta*, *Cymbaxinella damicornis* and *Cymbaxinella verrucosa* [13]. But in this work the authors have added a mixture of eight radiotracers simultaneously (^{110m}Ag, ^{241}Am, ^{109} Cd, ^{60}Co, ^{134}Cs, ^{54}Mn, ^{75}Se and ^{65}Zn) with [^{241}Am(III)] = $6.5x10^{-12}$ M. For a total period of around 80 h, the concentration factors (CF) obtained varied between 100 and 400 (CF is the ratio between radiotracer activity in the sponge (Bq/g) and the radiotracer activity in seawater (Bq/g)). In this work, for *A. cavernicola*, CF were measured around 830 and 1040 thus confirming previous results that tubular sponges and the present study *A. cavernicola* are accumulating species (keeping in mind that experiment has been taken place at the ultra-trace scale). However comparison with other concentration factors obtained in natural or semi natural conditions is difficult since CF are highly dependent on the chemical element itself (the chemistry of copper, cadmium or americium for instance are very different) and on the speciation and concentration of this element [16,

62]. In summary it can be asserted here that the americium complex present in seawater is taken up by the sponge and of the two specimens tested in this study, none of them died during the experiment.

In order to study the transfer mechanisms and to explain the presence of americium in sponge, the speciation of the radioelement in seawater has been further assessed. Americium belongs to the second half of the actinide series although it shares with the lighter elements the possibility of forming high valence species. Nonetheless, the chemistry of americium is mostly governed by the +III oxidation state in non-strongly oxidizing conditions. From this point of view, americium, curium and heavier actinides share with the lanthanide elements (except cerium) a certain chemical analogy although this assertion must always be taken with caution. Because the specific activity of americium (all isotopes) is relatively high, investigation on model systems with a chemical surrogate (here europium) is necessary to pinpoint the molecular speciation of the americium element in seawater. To our knowledge, this is the first attempt to document the molecular structure of this element in an environmentally relevant system.

3.2. Speciation modeling of americium (and europium) in seawater

The presence of numerous cations and anions, as well as organic matter (humic substances), in seawater (Table 1) forms a complex matrix. Sulphate, carbonate and hydroxide anions together with humic substances are the main species that can affect speciation [65, 66]. In any case, the environmental concentration of actinides in seawater due to anthropogenic activities is very low (except for uranium). Table 2 presents the average actinide concentrations in seawater [20] together with the specific case of the Mediterranean sea [1]. Americium mainly comes from atmospheric fall out of nuclear tests (1945-1980 period) and is present at concentrations below pM levels [66].

The results of speciation calculations of americium(III) at $5x10^{-5}$ M in seawater taking into account the different anion and cation concentrations from Table 1 are shown in Figure 2a. The speciation of americium(III) suggests that the predominant species expected in those conditions are $Am(CO_3)^+$, $Am(CO_3)_2^-$, $AmSO_4^+$ and $Am(OH)_2^+$ as already reported in various studies[1, 67, 68]. For comparison, the

europium(III) surrogate at [Eu] = $5x10^{-5}$ M in seawater (Figure 2b), follows the same trend. Indeed, $EuCO_3^+$, $Eu(CO_3)_2^-$ and $Eu(OH)_2^+$ were suggested as the predominant species in seawater, especially $EuCO_3^+$. However, in the case of americium the proportion of each species is not the same compared with europium. Indeed, in the case of europium, the predominant species is $EuCO_3^+$ at around 80 % whereas for americium $AmCO_3^+$ is the main species with 55 %. The contribution of other species is higher in the case of americium where the amount of Am^{3+} is not as high (< 10%). As a conclusion the speciation is more scattered in the case of americium.

3.3. Americium in seawater, EXAFS analysis

The EXAFS spectrum of americium(III) in doped seawater at $5x10^{-5}$ M was recorded. Figures 3a and 3b show the experimental EXAFS spectra of americium and corresponding Fourier transform. The use of a bidentate monocarbonate model (including the triple scattering path for a bidentate carbonate ligand) as suggested by the speciation modeling led to a bad adjustment of the spectrum in the R+Φ = 2.93 Å range. The study of the imaginary part of the Fourier transform obtained with this conformation reveals this divergence (see Supplementary Information, Figure S6). Alternatively, the use of a quadruple scattering path for a monodentate carbonate led to a better fit as shown in Figure S6. But a contribution is still clearly missing in the adjusted curve at R+Φ = 2.9 and 3.1 Å on the Fourier transform.

In order to go beyond this first and unsatisfactory approach, investigations were performed with the europium surrogate at $5x10^{-5}$ M. As already mentioned, at this concentration the solubility limit is observed for europium, and a mixture of soluble and solid phases is present in the solution whereas no precipitate is observed in the case of americium. Indeed, the solubility of americium carbonate complexes is usually reported to be slightly higher than that of europium. For example, in the case of $M_2(CO_3)_3$ and $NaM(CO_3)_2.5H_2O$ the solubility product is lower than in the case of europium with log Ks equal to -31.78 and -17.5 for europium and -29.45 and -16.5 for americium respectively[39, 40]. Nevertheless, the use of

europium as a surrogate for complementary model studies is essential for better understanding the unexplained scattering contributions observed in the EXAFS spectrum of americium in seawater.

3.4. Speciation of the europium surrogate in seawater, soluble an solid phases

Europium has a characteristic luminescence spectrum in the red which makes it an ideal element for TRLIF with its strongest lines around 580, 593, 617, 650 and 700 nm ($^5D_0 \rightarrow {}^7F_J$ J= 0 – 4) [35, 69]. The main fluorescent wavelengths used are at 593 nm and the hypersensitive ($^5D_0 \rightarrow {}^7F_2$) at 617 nm together with 580 nm. Characteristics shifts in the peak maxima and intensities of the hypersensitive band change significantly upon coordination. Table 3 summarizes the spectroscopic data (main luminescence wavelengths, mean full width at mid height and lifetime) obtained in this study for the $5x10^{-5}$ doped sample compared with literature data.

The spectrum of a standard solution of europium(III) in acidic conditions is characteristic of the aquo species (Figure 4) with a higher intensity at 593 nm than at 617 nm. As expected, in the dissolved phase of Eu doped seawater, [Eu(III)] = (6.1 ± 0.2) $x10^{-7}$ M, the intensity of the hypersensitive band is enhanced as an indication of complexation (Figure 4). The spectrum of this solution phase presents three peaks at 580, 593 and 616 nm. The peak ratio I_{593}/I_{616} is 1:3 and the luminescence lifetime is 140 ± 10 µs. This peak ratio suggests the major presence of a biscarbonate species, $Eu(CO_3)_2^-$ [35, 69]. In previous studies, the europium biscarbonate lifetime is reported at 290 ± 30 µs for a carbonate solution prepared in K_2CO_3[69] and at 140 ± 10 µs [35] for a carbonate solution prepared in natural water with a significant amount of sodium (0.02 M) compared to europium ($5x10^{-6}$ M). The low value obtained in this study could therefore be explained by the presence of sodium. From the lifetime value the number of water molecules around europium has been derived using the following equation[69] : $n_{H_2O} \pm 0.5 = \frac{1.07}{\tau} - 0.62$, where τ is in ms. Hence, in seawater, the derived number of water molecules around europium is equal to 7. Moreover, the peak at 580 nm is more intense in the solution phase than in the solid phase. This peak corresponds to the transition $^5D_0 \rightarrow {}^7F_0$ and is known to increase when symmetry decreases [70]. One

possibility is that in solution the electrostatic attraction between Na^+ and $Eu(CO_3)_2^-$ must be screened compared to the solid and more movements may occur, thus explaining the decrease in symmetry.

The spectrum of the particulate phase also exhibits the same three peaks with a peak ratio I_{593}/I_{617} of 1 : 3 (Figure 4) corresponding to the biscarbonate species. However two lifetimes, a very short one at 6 ± 1 µs and a longer one at 99 ± 10 µs have been observed. This suggests that two different europium environments are present and could result from two isomeric forms upon precipitation with possible cross relaxation because the second lifetime is very short. Previous studies have already reported that the complexation between europium and carbonate ligands in aqueous solution is governed by equilibration between a precipitate and a soluble phase and this process requires at least two days [71-73]. Lanthanide(III) (and actinide(III)) carbonates are complex binary or ternary systems that are governed by the carbonate concentration, the pH, the ionic strength and the presence of other cations (usually alkaline). Hence, in the case of europium, with a high ionic strength (NaCl or $NaClO_4$) and high carbonate concentration (> 10^{-3} M) the limiting carbonate complex, $Eu(CO_3)_3^{3-}$, was observed in solution in equilibrium with $NaEu(CO_3)_2.nH_2O$ in solid phase [40, 72] [41]. It has been shown that when the carbonate concentration is lower than 0.003 M, $Eu(CO_3)_3^{3-}$ is not formed in solution but the alternative complex is not known [72] and is in equilibrium with $NaEu(CO_3)_2.nH_2O$. To summarize, the peak ratio I_{593}/I_{617} in solution and solid phases being the same (1 : 3) this suggests that the biscarbonate species is most likely present both in the solution phase and in the solid phase. However, the lifetimes are significantly different between the solution and the solid phase and this may be attributed to a possible influence of isomerism (as suggested form the variation of the peak at 580 nm).

In order to assess the impact of the presence of sodium, complementary structural data with solid state ATR-FTIR was obtained on the solid phase. The following solids were compared: solid phase obtained directly from doped seawater after 2 days, $Eu_2(CO_3)_3.nH_2O$[39] and as prepared from europium and carbonate in NaCl solution at seawater concentrations (see experimental section). The IR spectra are compared in Figure 5. In each case, the characteristic asymmetric and symmetric bands ν_3 of the CO_3^{2-} groups at 1504 and 1370 cm^{-1} are well distinguished, thus confirming the presence of carbonate ligands in

the 3 species [39]. Previous studies have shown that the symmetry of the carbonate affects the value of $\Delta\nu_3$: that is lower for a monodentate carbonate complex (80 – 120 cm^{-1}) than for a bidentate one (100 - 350 cm^{-1}). In addition, this value may also be affected by the cation and its charge [37, 38]. $\Delta\nu_3$ decreases when the ratio z/r^2 decreases, where z is the charge and r the ionic radius. For instance in the case of bidentate dicarbonato lanthanide complex, $NaLn(CO_3)_2$, $\Delta\nu_3$ lies in the range 100 – 140 cm^{-1}. In the seawater solid phase, the energy splitting between the two bands is 134 cm^{-1} which is in perfect agreement with the values reported for $NaLn(CO_3)_2$ with bidentate complexation. Moreover, comparison between the carbonate model $Eu_2(CO_3)_3.nH_2O$ and the seawater solid phase pinpoints a sharp band in the case of seawater at 638 cm^{-1}. Only the direct precipitation of europium carbonate in NaCl lead also to the presence of this band. This is a clear confirmation that Na is part of the structure of the europium carbonate formed in the solid phase in natural seawater.

In order to complement the results obtained by TRLIF suggesting the presence of two spatial arrangements in the solid phase (two lifetimes), the europium seawater solution was deposited onto a carbon disk and analyzed by SEM. SEM images together with EDX spectra revealed the presence of two forms (Figure 6). Indeed, Figure 6a shows a structured form with a stick appearance. This contrasts with the forms shown in Figure 6b which appears more amorphous with a spherical shape. In each case the elementary composition is the same, confirming the presence of sodium at the spots where europium is found as already determined by ICP-OES (the Eu:Na ratio is equal to 1:1, see experimental section).

These macroscopic images from precipitation confirm the presence of sodium and suggest the occurrence of isomeric forms in equilibrium at this concentration between the solution and the solid. It can therefore be assumed that all the species in equilibrium in the seawater solution at [Eu] = $5x10^{-5}$ M and then in the precipitate are isomeric forms of the ternary Eu-Na-CO_3 complex.

Finally the EXAFS spectrum of europium at $5x10^{-5}$ M in seawater and corresponding Fourier transform are presented in Figures 3a and 3b. According to the above observations, all the species in equilibrium in seawater were probed at the same time in the EXAFS cell. Therefore 2 bidentate carbonates were

considered in the first coordination sphere. An attempt to adjust the spectrum considering 2 monodentate carbonates led to a worse fit. Interestingly, the region between R+Φ = 2.7 and 3.3 Å can only be adequately reproduced (especially the contribution around R+Φ = 3.1 Å) by considering a Eu....Na scattering path. For comparison, the imaginary part of the FT with and without this path is shown in Figure S7 of Supplementary Information. The overall EXAFS best fit parameters reported in Table 4 are in remarkable agreement with the interpretation given above with TRLFS and ATR-FTIR. It results from the EXAFS data analysis that all these species in equilibrium belong to the ternary system Na-Eu-CO_3 as suggested above. The best metrical parameters (2.45(1) Å for Eu-O, 3.45(4) Å for Eu-Na, 4.15(1) Å for Eu…O_{dist}) are in good agreement with distances found in literature for europium carbonate $NaEu(CO_3)_2.5H_2O$ and for $Na_3Eu(CO_3)_3$ (2.46 Å for Eu-O, Eu-O_{dist} are 4.22 Å and 3.61 Å for Eu-Na) [41, 74]. The coordination number associated with the Eu…O_{dist} contributions obtained with the fit corresponds to the presence of two carbonate groups around europium. Moreover, the coordination number for Eu...Na matches remarkably with the ratio Eu: Na found with elementary analysis (1:1 see experimental section). One can note however that the total coordination number derived from TRLFS lies between 10.5 and 11.5 (this corresponds to 7 ± 0.5 water molecules plus two bidentate carbonate groups). This is not in full agreement with the total coordination number (9 ± 1) derived from the EXAFS adjustments. First of all the number of water molecules was obtained for the solution phase and may differ slightly in the solid phase. The concentration of europium in the solution being very low (below 10^{-6} M), the EXAFS spectrum is strongly influenced by the solid phase. Second, it is well known that estimation of the amplitude factors with EXAFS is very difficult in the absence of adequate experimental model systems and an error of 10-20% is commonly admitted.

3.5. Comparison between europium and americium speciation in doped seawater

The above data gathered on the europium seawater system show the occurrence of a ternary Eu-Na-CO_3 complex, both in solution and in solid phases, with the presence of different conformations. In particular,

the presence of Na in the structure is asserted. This new model was therefore implemented for the EXAFS data fitting of americium. Figure 3a and 3b show the EXAFS spectra of americium and corresponding Fourier transform. The best fit parameters are listed in Table 4. The best EXAFS metrical parameters are 2.48(1) Å for Am-O, 3.25(5) Å for Am…Na and 3.73(3) Å for Am…C. The study of the imaginary part of the Fourier transforms reveals that only the presence of sodium with two monodentate carbonate groups lead to the best adjustment of the spectrum with a good phase and amplitude (see Figure S6 of Supplementary information). In summary, for americium and europium, a biscarbonato complex with sodium was confirmed, one seems to be with two monodentate carbonates (Am) and the other with two bidentate carbonates (Eu). The formula of both complexes can be tentatively written as $NaAm(CO_3)_2.nH_2O$ and $NaEu(CO_3)_2.nH_2O$ respectively. This result differs slightly from the speciation modeling which suggested the presence of monocarbonate species. The presence of a monocarbonate complex cannot be excluded except in minor proportions.

4. Conclusion

In order to fully describe the transfer mechanisms of possible actinide element dissemination in the hydrosphere, marine compartment and biotope, knowledge of the chemical speciation of the element is compulsory. This report focuses on the speciation of americium(III) in seawater and sponging up by *A. cavernicola* as a model for accumulation tests. The study of the accumulation of americium at the ultra-trace level (0.72 pg/ml) in the sponge *A. cavernicola* indicates that americium is accumulated by the sponge with a linear trend. This suggests that *A. cavernicola* can accumulate americium under the present speciation. In order to better understand the sponging up of americium, knowledge of the speciation of this element in seawater is needed. Although the inventory of radionuclides, including actinide elements (uranium, plutonium, americium …) has been widely studied in seawater, direct speciation has been difficult to assess in the past, if not impossible, mostly because those elements are present at ultra-trace levels (below the ppb level) in the absence of hot contamination spots. The need for speciation data and further bioavailability is therefore dramatically lacking. In this report, direct speciation of americium in

doped seawater was assessed for the first time using Extended X-ray Absorption Fine Structure (EXAFS). Because of the relatively high specific radioactivity of americium, europium was also used as a chemical surrogate for model systems. With a combination of Time-Resolved Laser-Induced Fluorescence (TRLIF), Extended X-ray Absorption Fine Structure (EXAFS), Scanning Electron Microscopy (SEM) and Attenuated Total Reflectance Fourier Transform Infrared (ATR-FTIR) spectroscopy, the speciation of europium in seawater was explored and used to fine tune the study on the americium case. For europium(III), in the same doping conditions as for americium ($5x10^{-5}$ M), two phases are in equilibrium. In both solid and liquid phases, it can be assumed that all the species in equilibrium are isomeric forms of the ternary Eu-Na-CO_3 complex, most likely the sodium biscarbonato complex, $NaEu(CO_3)_2.nH_2O$. In the solid complex, bidentate carbonates are present. In the case of americium(III), the EXAFS data also indicates the presence of the ternary Am-Na-CO_3 complex as the main species in solution with clear evidence of the contribution of sodium cations in the structure. In this complex (by analogy $NaAm(CO_3)_2.nH_2$), the carbonate ligands seem to be monodentate in contrast with the europium case.

Further studies have yet to be conducted in order to assess the bio or chemical transformation of the carbonato complex americium upon absorption by marine organisms. The present study confirms the importance of speciation, not only for the better understanding of the transfer mechanisms from the hydrosphere to the biosphere but also for the evaluation of the impact on humans via the food chain or on the environment and biota.

Acknowledgements

This work was jointly financed by the DPN (Direction of Naval Propulsion) CEA/DAM and CNRS / Institut National de Chimie. The experimental work using sponges was conducted by the author M.M. under an internship at the IAEA-Environment Laboratories in Monaco. The International Atomic Energy Agency is grateful to the Government of the Principality of Monaco for the support provided to its Environment Laboratories. XAS experiments were performed at the MARS beam line of SOLEIL

synchrotron, Gif sur Yvette, France. The authors would like to thank Andrew Dick (Edinburgh Instrument) for implementing the TRLIF instrument with specific capacities. We would like to thank laboratories (LEAV, Laboratoire de l'Environnement et de l'Alimentation de la Vendée, LASAT, Laboratoire d'Analyses Sèvres Atlantique and PROTEE, PROcessus de Transferts et d'Echanges dans l'Environnement) which performed the analysis of seawater. The authors wish to thank Olivier Marie (CEA- DAM) for SEM measurements.

REFERENCES

1. Atwood, D.A., *Radionuclides in the Environment*. 2013: John Wiley & Sons.
2. Hu, Q.-H., J.-Q. Weng, and J.-S. Wang, *Sources of anthropogenic radionuclides in the environment: a review.* Journal of Environmental Radioactivity, 2010. **101**(6): p. 426-437.
3. Le Petit, G., et al., *Analysis of Radionuclide Releases from the Fukushima Dai-Ichi Nuclear Power Plant Accident Part I.* Pure and Applied Geophysics, 2014. **171**(3-5): p. 629-644.
4. Kirishima, A., et al., *Leaching of actinide elements from simulated fuel debris into seawater.* Journal of Nuclear Science and Technology, 2015: p. 1-7.
5. Achim, P., et al., *Analysis of Radionuclide Releases from the Fukushima Dai-ichi Nuclear Power Plant Accident Part II.* Pure and Applied Geophysics, 2012. **171**(3-5): p. 645-667.
6. Oikawa, S., T. Watabe, and H. Takata, *Distributions of Pu isotopes in seawater and bottom sediments in the coast of the Japanese archipelago before and soon after the Fukushima Dai-ichi Nuclear Power Station accident.* Journal of Environmental Radioactivity, 2015. **142**: p. 113-123.
7. Periáñez, R., et al., *A comparison of marine radionuclide dispersion models for the Baltic Sea in the frame of IAEA MODARIA program.* Journal of Environmental Radioactivity, 2015. **139**: p. 66-77.
8. Neff, J.M., *Bioaccumulation in marine organisms: effect of contaminants from oil well produced water*. 2002: Elsevier.
9. Mason, R., J.-M. Laporte, and S. Andres, *Factors controlling the bioaccumulation of mercury, methylmercury, arsenic, selenium, and cadmium by freshwater invertebrates and fish.* Archives of Environmental Contamination and Toxicology, 2000. **38**(3): p. 283-297.
10. Boening, D.W., *An evaluation of bivalves as biomonitors of heavy metals pollution in marine waters.* Environmental monitoring and assessment, 1999. **55**(3): p. 459-470.
11. Nelson, W.G., B.J. Bergen, and D.J. Cobb, *Comparison of PCB and trace metal bioaccumulation in the blue mussel, Mytilus edulis, and the ribbed mussel, Modiolus demissus, in new Bedford Harbor, Massachusetts.* Environmental toxicology and chemistry, 1995. **14**(3): p. 513-521.
12. Roditi, H.A., N.S. Fisher, and S.A. Sañudo-Wilhelmy, *Field testing a metal bioaccumulation model for zebra mussels.* Environmental science & technology, 2000. **34**(13): p. 2817-2825.
13. Genta-Jouve, G., et al., *Comparative bioaccumulation kinetics of trace elements in Mediterranean marine sponges.* Chemosphere, 2012. **89**: p. 340-349.
14. Patel, B., M. Balani, and S. Patel, *Sponge 'sentinel'of heavy metals.* Science of the total environment, 1985. **41**(2): p. 143-152.
15. de Mestre, C., et al., *Sponges as sentinels: patterns of spatial and intra-individual variation in trace metal concentration.* Mar Pollut Bull, 2012. **64**(1): p. 80-9.

16. Cebrian, E., M.J. Uriz, and X. Turon, *Sponges as biomonitors of heavy metals in spatial and temporal surveys in northwestern Mediterranean: multispecies comparison.* Environmental Toxicology and Chemistry, 2007. **26**(11): p. 2430-2439.
17. Vacelet, J., *Répartition générale des éponges et systématique des éponges cornées de la région de Marseille et de quelques stations méditérrannéennes*. 1959.
18. Noshkin, V.E., *Concentrations and concentration factors of several anthropogenic and natural radionuclides in marine vertebrates and invertabrates.* 1984.
19. Buesseler, K.O., et al., *Fukushima-derived radionuclides in the ocean and biota off Japan.* Proceedings of the National Academy of Sciences, 2012. **109**(16): p. 5984-5988.
20. Choppin, G.R., *Actinide speciation in aquatic systems.* Marine Chemistry, 2006. **99**(1-4): p. 83-92.
21. Konstantinou, M. and I. Pashalidis, *Speciation and spectrophotometric determination of uranium in seawater.* Mediterranean Marine Science, 2004. **5**(1): p. 55 - 60.
22. Morcillo, F., et al., *Biosorption and biomineralization of U(VI) by the marine bacterium idiomarina loihiensis MAH1: Effect of background electrolyte and pH.* PLoS ONE, 2014. **9**(3): p. e91305.
23. Guillaumont, R. and F.J. Mompean, *Update on the chemical thermodynamics of uranium, neptunium, plutonium, americium and technetium.* 2003.
24. Sakaguchi, A., et al., *Isotopic determination of U, Pu and Cs in environmental waters following the Fukushima Daiichi Nuclear Power Plant accident.* Geochemical Journal, 2012. **46**: p. 335 - 360.
25. Hirose, K. and M. Aoyama, *Chemical speciation of plutonium in seawater.* Analytical and Bioanalytical Chemistry, 2002. **372**(3): p. 418-420.
26. Maxwell, S., et al., *Rapid determination of actinides in seawater samples.* Journal of Radioanalytical and Nuclear Chemistry, 2014. **300**(3): p. 1175-1189.
27. LoPresti, V., S.D. Conradson, and D.L. Clark, *XANES identification of plutonium speciation in RFETS samples.* Journal of Alloys and Compounds, 2007. **444-445**(0): p. 540-543.
28. Prat, O., et al., *Uranium speciation in drinking water from drilled wells in southern finland and its potential links to health effects.* Environmental Science & Technology, 2009. **43**(10): p. 3941-3946.
29. Ansoborlo, E., L. Lebaron-Jacobs, and O. Prat, *Uranium in drinking-water: A unique case of guideline value increases and discrepancies between chemical and radiochemical guidelines.* Environ Int, 2015. **77C**: p. 1-4.
30. Maloubier, M., et al., *XAS and TRLIF spectroscopy of uranium and neptunium in seawater.* Dalton Transactions, 2015. **44**: p. 5417-5427.
31. Silva, R. and H. Nitsche, *Actinide environmental chemistry.* Radiochimica Acta, 1995. **70**(71): p. 377-396.
32. Berthoud, T., et al., *Direct uranium trace analysis in plutonium solutions by time-resolved laser-induced spectrofluorometry.* Analytical Chemistry, 1988. **60**(13): p. 1296-1299.
33. Fujimori, H., T. Matsui, and K. Suzuki, *Simultaneous Determination of Uranium and HNO3 Concentrations in Solution by Laser-Induced Fluorescence Spectroscopy.* Journal of Nuclear Science and Technology, 1988. **25**(10): p. 798-804.
34. Moulin, C., P. Decambox, and P. Mauchien, *State of the art in time-resolved laser-induced fluorescence for actinides analysis: Applications and trends.* Journal of Radioanalytical and Nuclear Chemistry, 1997. **226**(1-2): p. 135-138.
35. Moulin, C., et al., *Europium complexes investigations in natural waters by time-resolved laser-induced fluorescence.* Analytica Chimica Acta, 1999. **396**(2-3): p. 253-261.

36. Sundman, A., T. Karlsson, and P. Persson, *An experimental protocol for structural characterization of Fe in dilute natural waters.* Environmental Science & Technology, 2013. **47**(15): p. 8557-8564.
37. Jolivet, J.P., et al., *Infrared spectra of cerium and thorium pentacarbonate complexes.* Journal of Molecular Structure, 1982. **79**(0): p. 403-408.
38. Hiemstra, T., R. Rahnemaie, and W.H. van Riemsdijk, *Surface complexation of carbonate on goethite: IR spectroscopy, structure and charge distribution.* Journal of Colloid and Interface Science, 2004. **278**(2): p. 282-290.
39. Runde, W., G. Meinrath, and J.I. Kim, *A study of solid-liquid phase equilibria of trivalent lanthanide and actinide ions in carbonate systems.* Radiochim. Acta, 1992. **58-59**(Pt. 1): p. 93-100.
40. Vercouter, T., et al., *Eu(CO3)33- and the limiting carbonate complexes of other M3+ f-elements in aqueous solutions: a solubility and TRLFS study.* New Journal of Chemistry, 2005. **29**(4): p. 544-553.
41. Runde, W., C. Van Pelt, and P.G. Allen, *Spectroscopic characterization of trivalent f-element (Eu-Am) solid carbonates.* Journal of Alloys and Compounds, 2000. **303-304**: p. 182-190.
42. Van der Lee, J., *JCHESS version 2.0. École des Mines de Paris, Centre d'information géologique, 2000–2001*. 2010.
43. Bion, L., *BASSIST: an applied thermodynamic database for radionuclide chemistry.* Radiochimica Acta, 2003. **91**(11): p. 633-637.
44. Van der Lee, J., *CHESS, another speciation and surface complexation computer code.* CIG-Ecole des Mines de Paris, 1993.
45. Nolting, R., et al., *Cadmium, copper and iron in the Scotia Sea, Weddell Sea and Weddell/Scotia Confluence (Antarctica).* Marine Chemistry, 1991. **35**(1): p. 219-243.
46. Nolting, R.F. and H.J.W. de Baar, *Behaviour of nickel, copper, zinc and cadmium in the upper 300 m of a transect in the Southern Ocean (57°–62°S, 49°W).* Marine Chemistry, 1994. **45**(3): p. 225-242.
47. Saager, P.M., H.J.W. De Baar, and R.J. Howland, *Cd, Zn, Ni and Cu in the Indian Ocean.* Deep Sea Research Part A. Oceanographic Research Papers, 1992. **39**(1): p. 9-35.
48. Noakes, J.E. and D.W. Hood, *Boron-boric acid complexes in sea-water.* Deep Sea Research (1953), 1961. **8**(2): p. 121-129.
49. Robertson, D.E., *The distribution of cobalt in Oceanic waters.* Geochimica et Cosmochimica Acta, 1970. **34**(5): p. 553-567.
50. Schaule, B. and C. Patterson, *Perturbations of the Natural Lead Depth Profile in the Sargasso Sea by Industrial Lead*, in *Trace Metals in Sea Water*, C.S. Wong, et al., Editors. 1983, Springer US. p. 487-503.
51. Wong, G.T.F. and X.-H. Cheng, *Dissolved organic iodine in marine waters: Determination, occurrence and analytical implications.* Marine Chemistry, 1998. **59**(3–4): p. 271-281.
52. Quinby-Hunt, M.S. and K.K. Turehian, *Distribution of elements in sea water.* Eos, Transactions American Geophysical Union, 1983. **64**(14): p. 130-130.
53. Mason, R.P., K.R. Rolfhus, and W.F. Fitzgerald, *Mercury in the North Atlantic.* Marine Chemistry, 1998. **61**(1–2): p. 37-53.
54. Ólafsson, J., *Mercury Concentrations in the North Atlantic in Relation to Cadmium, Aluminium and Oceanographic Parameters*, in *Trace Metals in Sea Water*, C.S. Wong, et al., Editors. 1983, Springer US. p. 475-485.
55. Measures, C.I., *The distribution of Al in the IOC stations of the eastern Atlantic between 30 ° S and 34 ° N.* Marine Chemistry, 1995. **49**(4): p. 267-281.

56. LLorens, I., et al., *X-ray absorption spectroscopy investigations on radioactive matter using MARS beamline at SOLEIL synchrotron.* Radiochimica Acta, 2014.
57. Sitaud, B., et al., *Characterization of radioactive materials using the MARS beamline at the synchrotron SOLEIL.* Journal of Nuclear Materials, 2012. **425**(1–3): p. 238-243.
58. Ravel, B. and M. Newville, *ATHENA, ARTEMIS, HEPHAESTUS: data analysis for X-ray absorption spectroscopy using IFEFFIT.* Journal of synchrotron radiation, 2005. **12**(4): p. 537-541.
59. Michalowicz, A., et al. *MAX: multiplatform applications for XAFS*. in *Journal of Physics: Conference Series*. 2009. IOP Publishing.
60. Michalowicz, A., et al. *MAX (Multiplatform Applications for XAFS) New Features*. in *Journal of Physics: Conference Series*. 2013. IOP Publishing.
61. Rehr, J.J., et al., *Parameter-free calculations of X-ray spectra with FEFF9.* Physical Chemistry Chemical Physics, 2010. **12**(21): p. 5503-5513.
62. Cebrian, E., et al., *Response of the Mediterranean sponge Chondrosia reniformis Nardo to copper pollution.* Environ Pollut, 2006. **141**(3): p. 452-8.
63. Cebrian, E., et al., *Sublethal effects of contamination on the Mediterranean sponge Crambe crambe: metal accumulation and biological responses.* Marine Pollution Bulletin, 2003. **46**(10): p. 1273-1284.
64. Cebrian, E. and M.J. Uriz, *Contrasting effects of heavy metals on sponge cell behavior.* Arch Environ Contam Toxicol, 2007. **53**(4): p. 552-8.
65. Maher, K., J.R. Bargar, and G.E. Brown, *Environmental Speciation of Actinides.* Inorganic Chemistry, 2013. **52**(7): p. 3510-3532.
66. Choppin, G. and P. Wong, *The Chemistry of Actinide Behavior in Marine Systems.* Aquatic Geochemistry, 1998. **4**(1): p. 77-101.
67. Choppin, G.R., *Soluble rare earth and actinide species in seawater.* Marine Chemistry, 1989. **28**(1-3): p. 19-26.
68. Choppin, G.R. and B.E. Stout, *Actinide behavior in natural waters.* Science of The Total Environment, 1989. **83**(3): p. 203-216.
69. Plancque, G., et al., *Europium speciation by time-resolved laser-induced fluorescence.* Analytica Chimica Acta, 2003. **478**(1): p. 11-22.
70. Binnemans, K., *Interpretation of europium(III) spectra.* Coordination Chemistry Reviews, 2015. **295**: p. 1-45.
71. Philippini, V., et al., *Precipitation of ALn (CO3) 2, xH2O and Dy2 (CO3) 3, xH2O compounds from aqueous solutions for and.* Journal of Solid State Chemistry, 2008. **181**(9): p. 2143-2154.
72. Philippini, V., T. Vercouter, and P. Vitorge, *Evidence of different stoichiometries for the limiting carbonate complexes across the lanthanide(III) series.* Journal of solution chemistry, 2010. **39**(6): p. 747-769.
73. Cantrell, K.J. and R.H. Byrne, *Rare earth element complexation by carbonate and oxalate ions.* Geochimica et Cosmochimica Acta, 1987. **51**(3): p. 597-605.
74. Mercier, N., et al., *Structural and Optical Investigations of Sodium Europium Carbonate Na3Eu(CO3)3.* Journal of Solid State Chemistry, 1997. **132**(1): p. 33-40.

Table 1: Main physico-chemical parameters of. Data from LEAV, LASAT and PROTEE*.

pH	7.8 ± 0.8
E_h (18°C)	210 mV vs. NHE
Salinity	38 ± 2 g/kg
Cl^-	603 ± 60 mM
SO_4^{2-}	32 ± 5 mM
HCO_3^-	2.2 ± 0.2 mM
NO_3^-	0.0018 ± 0.0007 mM
PO_4^{3-}	0.0025 ± 0.0006 mM
Br^-	0.9 ± 0.2 mM
F^-	0.051 ± 0.008 mM
Na^+	560 ± 70 mM
Mg^{2+}	58 ± 7 mM
Ca^{2+}	11 ± 1 mM
NH_4^+	< 0.0004 mM
K^+	11 ± 1 mM
Sr^{2+}	0.10 ± 0.02 mM
Humic Substances	0.84 ± 0.08 mg/L

** LEAV, Rond-Point Georges Duval, BP 802,F-85021 La Roche sur Yon ; LASAT, 5 allée de l'océan, BP40355, F-17001 La Rochelle Cedex 1 ; PROTEE , University of Toulon-Var, BP 20132, F-83957 La Garde Cedex.*

Table 2: Radionuclides average concentration in seawater. Lines are shaded when no data were available.

Actinide (main isotope)	Average concentration (M) [20]	Concentration in Mediterranean (M)[1]
^{232}Th	$4.3\ 10^{-13}$	$< 3\ 10^{-12}$
^{238}U	$1.3\ 10^{-8}$	1.4 to $1.6\ 10^{-8}$
^{238}Pu	$3\ 10^{-18}$	
^{239}Pu	$1\ 10^{-14}$	$^{239,240}Pu \approx 10^{-17}$
^{240}Pu	$3\ 10^{-15}$	
^{241}Pu	$8\ 10^{-17}$	
^{241}Am	$4\ 10^{-17}$	5.10^{-20} to 10^{-19}
^{237}Np	$2\ 10^{-14}$	
^{90}Sr	$4.3.10^{-15}$	
^{137}Cs	4 to 7.10^{-18}	$5.7\ 10^{-18}$

Table 3: Spectroscopic data (fluorescence wavelengths, full width at mid height, lifetime) of europium in doped seawater and comparison with literature data.

Species	Fluorescence wavelengths (nm)	FWHM (nm)	Ratio 617 nm /593 nm	Lifetime (µs)	n H_2O	Ref
Seawater solution, [Eu] = 5 x 10^{-5} M	580-594-616	1.6/5.7/8.5	3	140 ± 10	7	This work
Seawater precipitate, [Eu] = 5 x 10^{-5} M	580-(592-597)-(616-620)	2.1/7.3/8.7	3	6 ± 1 µs 99 ± 10 µs	-	This work
Eu^{3+}	593-617	6.5/9.5	1/8	110 ± 10	9	[69]
$Eu(CO_3)^+$	580-591-616	3.2/11/10	2	180 ± 20	5	[69]
$Eu(CO_3)_2^-$	580-592-616	3.3/10/9	3	290±30	3	[69]
	580-(590-596)-(614-620)	4-9.5	3.1 ± 0.1	140 ± 10	7	[35]
$Eu(OH)^{2+}$	580-592-616	3.8/12/-	1	50±5	-	[69]
$Eu(OH)_2^+$	580-593-615	3.8/12/-	1	40 ± 5	-	[69]

Table 4: EXAFS best fit parameters for europium and americium in doped seawater. Numbers in italics have been fixed or linked. S_o^2 is the EXAFS global amplitude factor, e_o is the energy threshold, ε is the average noise and r(%) is the agreement factor of the fit.

	First shell	Second shell	Third shell [a]
Seawater solution, [Eu] = 5 x 10^{-5} M	*9* O at 2.46(1) Å	*1* Na at 3.45(5) Å	2.5(8) Odist at 4.15(1)Å
	σ^2 = 0.0128Å^2	σ^2 = 0.0040 Å^2	σ^2 = 0.0063 Å^2
	s_o^2 = 1.0, e_o = -1.81 eV, ε = 0.004, r(%) = 3.0		
Seawater solution, [Am] = 5 x 10^{-5} M	*9* O at 2.48(1)Å	*1* Na at 3.25(5) Å	*2* C at 3.73(3)
	σ^2 = 0.0094 Å^2	σ^2 =0.0094 Å^2	σ^2 = 0.0049 Å^2
	s_o^2 = 1.1, e_o = -5.83 eV, ε = 0.009, r(%) = 1.0		

[a] from Eu…C-O_{dist} triple path (O_{dist} = distal oxygen of carbonate) and Am…O-C-O quadruple path.

FIGURES CAPTION

Figure 1: Uptake curve of two *A. cavernicola* exposed to ^{241}Am dissolved in seawater.

Figure 2: Prediction speciation diagrams of americium at $5x10^{-5}$ M (a) and europium at $5x10^{-5}$ M (b) in seawater (JCHESS®)

Figure 2b: Europium speciation diagram (JCHESS®) in seawater at [Eu] = $5x10^{-5}$ M.

Figure 3a: Eu and Am L_{III} edge k^2-weighted EXAFS spectra of the doped seawater solution at [Eu,Am] = $5x10^{-5}$ M. Experimental spectra in black lines, adjustment in dots.

Figure 3b: Corresponding Fourier transform of the EXAFS spectrum of the doped seawater solution at $5x10^{-5}$ M. Experimental spectrum in black line, adjustment in dots.

Figure 4: TRLIF spectra: europium(III) standard solution (…) (pH 2), seawater soluble phase, [Eu] = 5x10-5 M (- -) (pH 7.8) and seawater, solid phase, [Eu] = 5x10-5 M (—) at 20 °C. Time delay 5 µs, aperture time 600 µs, number of accumulations 500 for the solution and 50 for the precipitate.

Figure 5: FTIR spectra of three solids: $Eu_2(CO_3)_3.nH_2O$, precipitate obtained in seawater and europium carbonate in NaCl.

Figure 6: SEM images and associated EDX spectra of the two europium solids (a, b) present in the doped seawater solution at [Eu]=$5x10^{-5}$ M after evaporation.

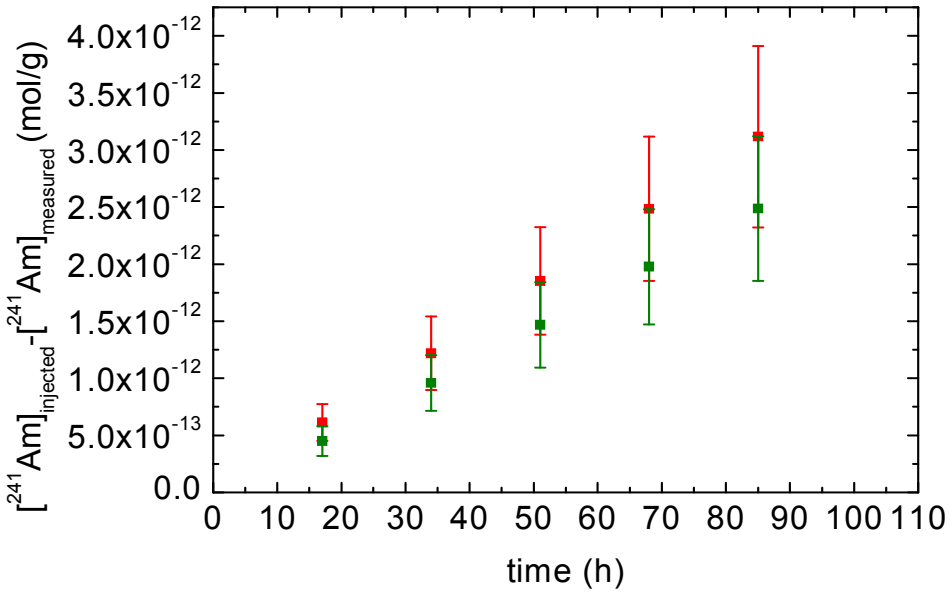

Figure 1: Uptake curve of two *A. cavernicola* exposed to ^{241}Am dissolved in seawater.

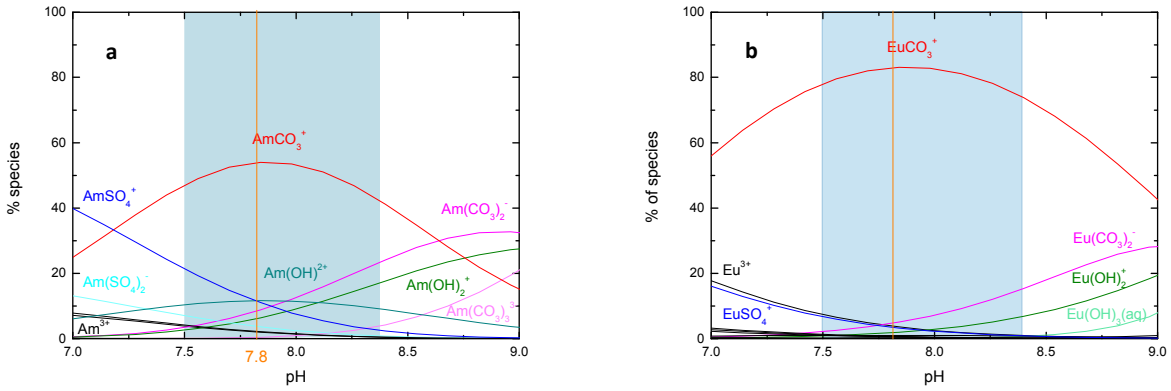

Figure 2: Prediction speciation diagrams of americium at 5x10^{-5} M (a) and europium at 5x10^{-5} M (b) in seawater (JCHESS®)

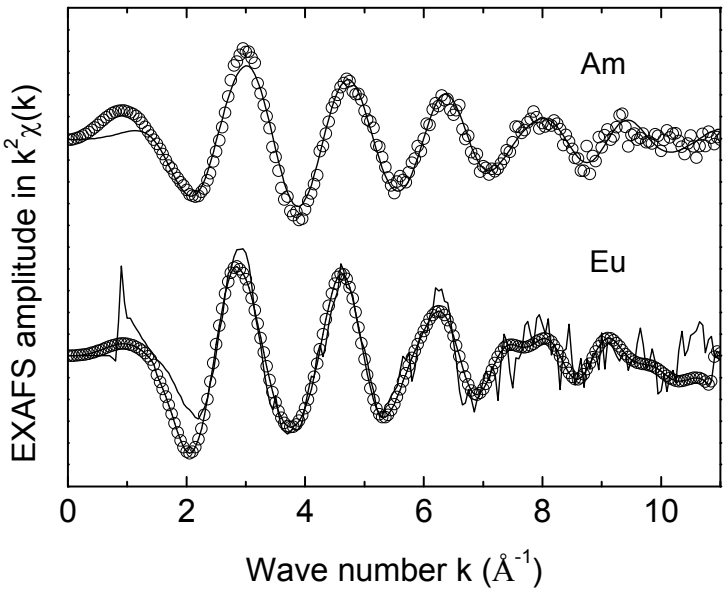

Figure 3a: Eu and Am L_{III} edge k^2-weighted EXAFS spectra of the doped seawater solution at [Eu,Am] = $5x10^{-5}$ M. Experimental spectra in black lines, adjustment in dots.

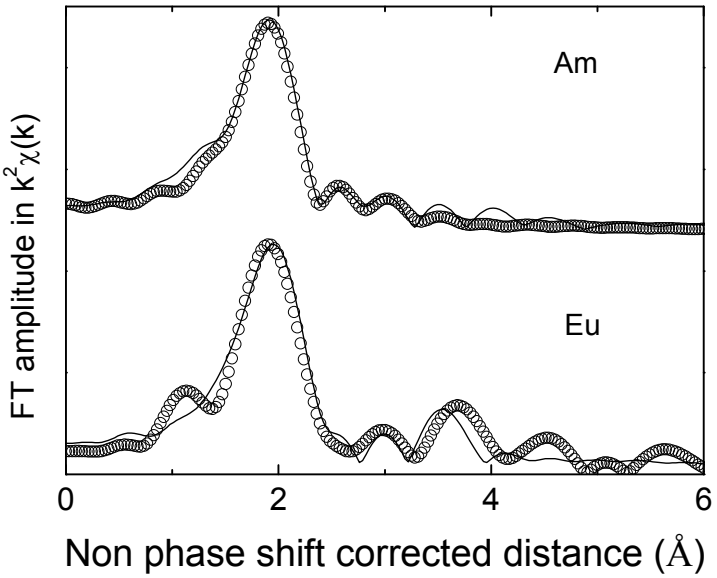

Figure 3b: Corresponding Fourier transform of the EXAFS spectrum of the doped seawater solution at $5x10^{-5}$ M. Experimental spectrum in black line, adjustment in dots.

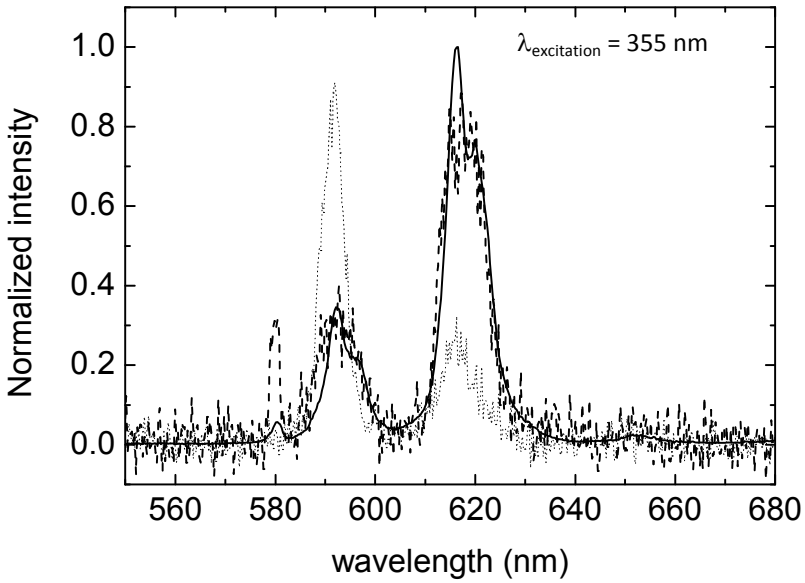

Figure 4: TRLIF spectra: europium(III) standard solution (…) (pH 2), seawater soluble phase, [Eu] = 5x10-5 M (- -) (pH 7.8) and seawater, solid phase, [Eu] = 5x10-5 M (—) at 20 °C. Time delay 5 µs, aperture time 600 µs, number of accumulations 500 for the solution and 50 for the precipitate.

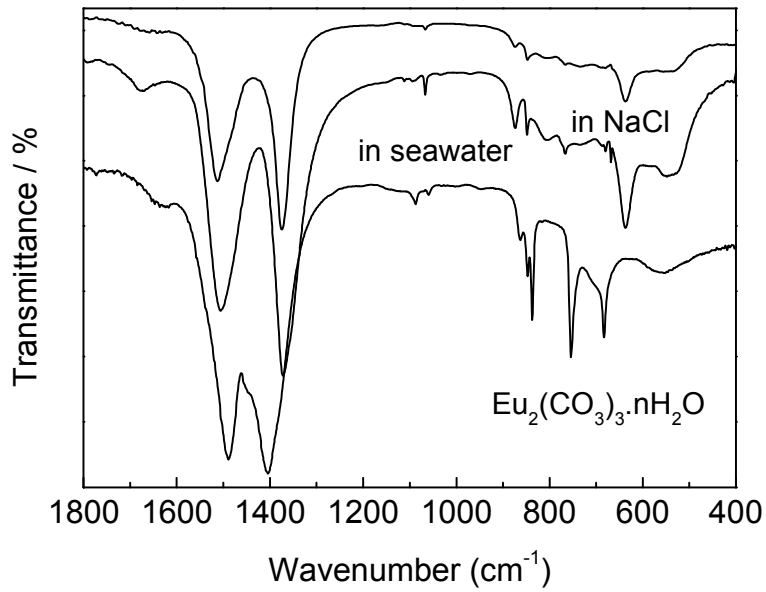

Figure 5: FTIR spectra of three solids: $Eu_2(CO_3)_3.nH_2O$, precipitate obtained in seawater and europium carbonate in NaCl.

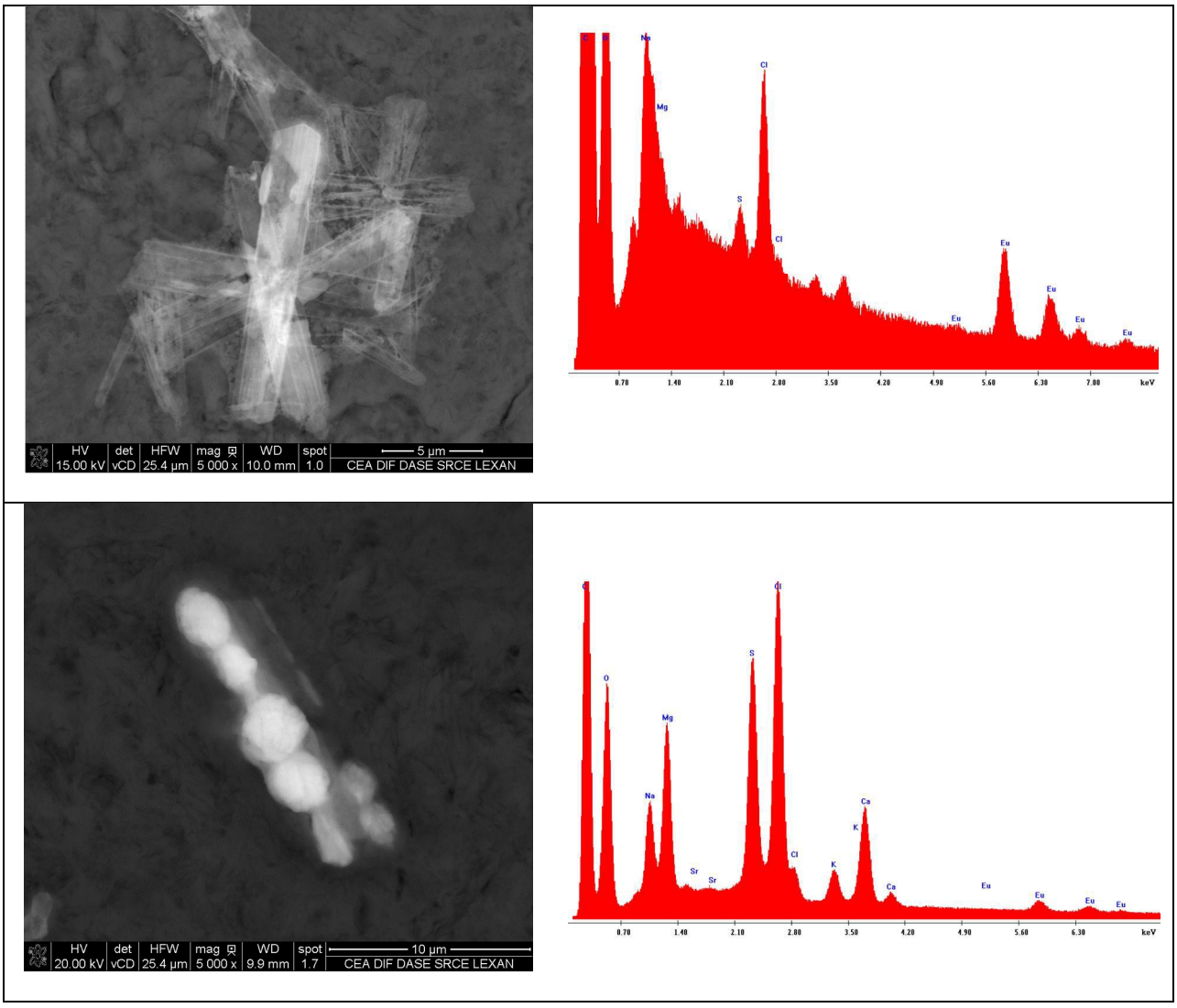

Figure 6: SEM images and associated EDX spectra of the two europium solids (a, b) present in the doped seawater solution at [Eu]=$5x10^{-5}$ M after evaporation.

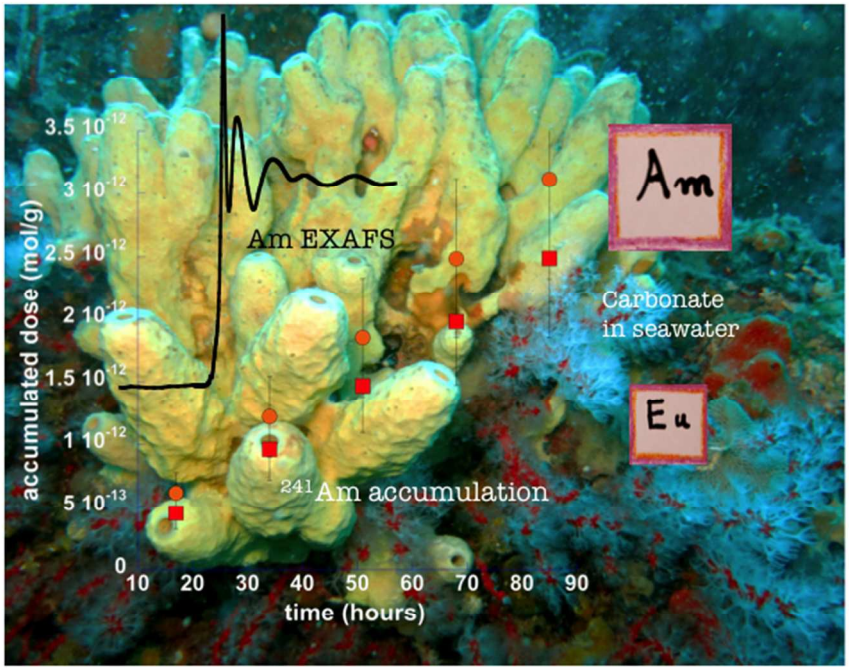

254x190mm (72 x 72 DPI)